Journal of Structural Geology 32 (2010) 975–981

Contents lists available at ScienceDirect

Journal of Structural Geology

journal homepage: www.elsevier.com/locate/jsg

Strain analysis from point fabric patterns: An objective variant of the Fry method

Richard J. Lisle

School of Earth and Ocean Sciences, Cardiff University, Cardiff CF10 3YE, United Kingdom

ARTICLE INFO

Article history:
Received 25 August 2009
Received in revised form
2 June 2010
Accepted 16 June 2010
Available online 23 June 2010

Keywords:
Strain analysis
Fry method
Statistical tests
Point patterns

ABSTRACT

A simple technique is devised for obtaining finite strain estimates from deformed patterns of points possessing anticlustered properties. As an alternative to the Fry approach where analysis is carried out in the deformed state, the new method performs a large number of trial de-strainings of the point pattern. For each de-strained dataset, a statistical analysis tests for the assumed properties of the point fabric in the pre-deformational state, that the points come from an isotropic but non-Poisson distribution. This computer-based procedure usually yields a number of acceptable solutions for the possible strain ellipse in the given geological situation. The variability of the strain estimates for a given dataset provides an assessment of the precision of the strain results.

Testing of the method with both synthetic and real datasets suggests that a best estimate for the strain ellipse is one corresponding to the centre of gravity on the Elliott strain plot. The performance of the new method compares favourably with existing Fry methods.

1. Introduction

Geological strain analysis requires geometrical information relating to the rock in its pre-deformational and deformed states. The entities that yield this information are referred to as strain markers. Some strain markers consist of individual objects with specific shape e.g. fossils, ooids, and sedimentary clast outlines. Other strain markers may consist of collections of objects with particular orientation patterns, e.g., preferred orientation patterns of muscovites in a sample of slate. However a problem arises where neither type of strain marker is present in the rock being analyzed. To overcome this, Ramsay (1967) recognized a third type of strain marker where the necessary geometrical information is provided by mutual spatial arrangements of objects in the rock. This led to the development of strain analysis techniques based on the distances of separation of point objects in sedimentary, metamorphic and igneous rocks (Ramsay, 1967, p. 195; Fry, 1979; Hanna and Fry, 1979).

The most popular of these inter-object distance techniques is the all-object separation method devised by Fry (1979). This is a strain method based on a polar plot of vectors depicting the separation of the centres of all possible pairs of objects. Assuming that pairs of adjacent objects were no closer than a certain threshold distance in the pre-deformation state, the plotted vectors of the inter-object distances in the deformed state will surround an elliptical region devoid of data points, the so-called vacancy field. If the threshold distance applies strictly, the elliptical region portrays directly the shape of the finite strain ellipse. The Fry method has been used to determine the finite strain in deformed clastic sedimentary rocks (Treagus and Treagus, 2002), in gneisses (Lacassin and van der Driessche, 1983), igneous rocks (Schwerdtner et al., 1983), etc. where grain centres provide the required object data. In addition, the method has been applied to deformed patterns of points not consisting of the centres of grains. Examples of such non-granular data used for Fry analysis are sand volcanoes (Waldron and Jensen, 1985).

For the majority of applications of the Fry method, the choice of the ellipse that best describes the periphery of the vacancy field is normally a source of ambiguity. This uncertainty arises where a strict inter-point threshold distance does not exist because neighbouring points show a weaker tendency for constant separation, i.e., a lesser degree of anticlustering. This spatial variability arises from the stochastic nature of the underlying processes that typically form the point patterns studied, which has motivated several refinements of the Fry method that attempt to compute the best-fit ellipse as an alternative to visual selection (Waldron and Wallace, 2007).

After an estimate of the finite strain has been obtained by selection of the best-fitting ellipse, a problem remains of assessing the robustness of this estimate (Crespi, 1986). This is because different pre-deformation point distributions show different degrees of anticlustering. In cases of strong anticlustering (Fig. 1a), the shape of the vacancy field should approximate closely to that of the strain ellipse (Fig. 1b). However, in cases of very weak anticlustering, where the undeformed distribution of points approaches that resulting from a random (Poisson) distribution

E-mail address: lisle@cardiff.ac.uk

0191-8141/$ – see front matter © 2010 Elsevier Ltd. All rights reserved.
doi:10.1016/j.jsg.2010.06.008

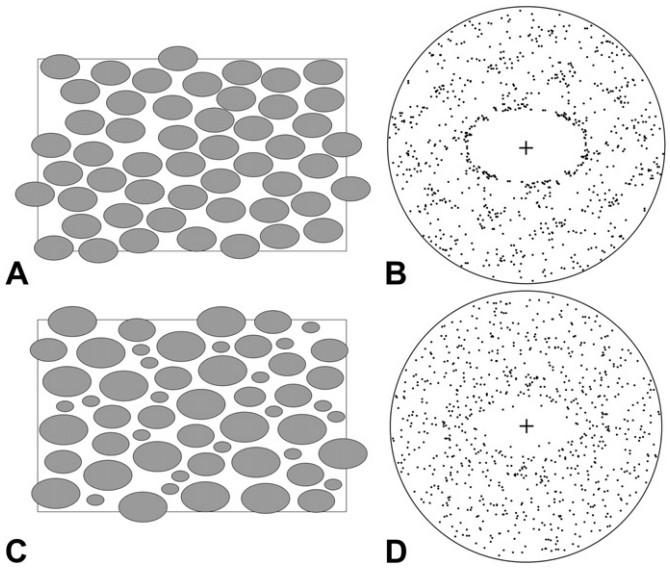

Fig. 1. Anticlustering and Fry plots. A, Grains in deformed rock with strongly anticlustered centres; B, corresponding Fry plot with well defined ellipse; C, Weakly anticlustered grain centres; D, corresponding Fry plot with poorly defined ellipse.

(Fig. 1c), the vacancy field in the deformed point pattern will have a size influenced by the number of points in the dataset and a shape that is largely independent of the applied strain (Fig. 1d). Although several methods have been suggested for determining the strain ellipse from point data, with the exception of McNaught (2002) for granular point data, none of these allows assessment of confidence limits for the obtained result.

The aim of this paper is to propose a new and simple method of strain analysis from point datasets of granular and non-granular types. The proposed method addresses both problems of subjectivity in obtaining a strain estimate, and the issue of qualifying the robustness of that estimate.

2. The assumptions of the method

The Fry plot has in the past been used as a display for a variety of types of spatial point patterns without necessarily a strain connotation. Examples are spatial distributions of mineralization (Vearncombe and Vearncombe, 1999) and of star clusters (Cartwright and Whitworth, 2008). Even when the point data are grain centres in a tectonite, the resulting elliptical Fry plot is not guaranteed to have a direct relationship to the finite strain ellipse. For this reason it seems advisable to generally refer to the Fry pattern as a descriptor of a point fabric ellipse rather than as the strain ellipse (Erslev, 1988). Only when the user is willing to make certain fundamental assumptions about the nature of the starting point patterns and of the imposed deformation, may the Fry plot be used to deduce the strain ellipse.

In this context, the proposed method determines the strain as an inverse problem; it uses the data from a deformed point distribution to constrain the principal parameters that had an influence on the final configuration of the deformed points. To estimate the magnitude and orientation of the finite strain ellipse, assumptions are made regarding the character of the strain and of the initial point distribution.

The assumptions concerning the strain are:

1) The strain is statistically homogeneous on scales ranging from that of the inter-point distances upward to the size of the overall area occupied by the sampled points. Smaller-scale heterogeneities in strain, such as those arising from the competence contrasts between grains and matrix, need not invalidate the method.
2) The strain history is coaxial, i.e. infinitesimal strains during the deformation are parallel to finite strains. This assumption is a cautionary one and is made to avoid special situations where strain may leave the original point configuration unaltered, e.g. the 'invisible' simple shear deformation of regular lattice patterns of points (Genier and Epard, 2007).

Concerning the initial point configuration, the pattern is assumed to be isotropic in the sense that distances between pair of points, whether immediate neighbours or not, do not vary systematically as a function of the orientation of the tie line. An example of such a population of point pairs is illustrated in a polar graph of the ends of vectors representing the lengths and orientations of the tie-lines drawn between all possible pairs of points in the sample (Fig. 2). Fry (1979) used this plot for the visual estimation of the strain ellipse. For the method, the plot is divided into three concentric hoop-shaped sampling cells. The assumption of isotropy means that a successful de-straining of the point data produces a uniform distribution of directions within each hoop-shaped sampling cell.

3. The method

Strain analysis using the proposed method involves a three-stage process. Firstly, data consisting of the coordinates of points in the deformed array are acquired and the inter-point vector (Fry) diagram constructed (Fig. 3a). Secondly, this dataset is subjected to a series of different geometrical transformations, each equivalent to a different retrodeformation of the point array (Fig. 3b).

This stage effectively subjects the dataset to a series of trial retrodeformations, each corresponding to the imposition of a strain ellipse with a particular axial ratio and orientation. In the final stage, the characteristics of each of the transformed datasets on the Fry plot are compared to those assumed for the pre-deformation configuration of the points (Fig. 3c, d). Where sufficient similarity exists, the corresponding trial retrodeformation is used to derive an acceptable solution of the finite strain parameters (Fig. 3d). The three stages of the method are performed by a FORTRAN 95

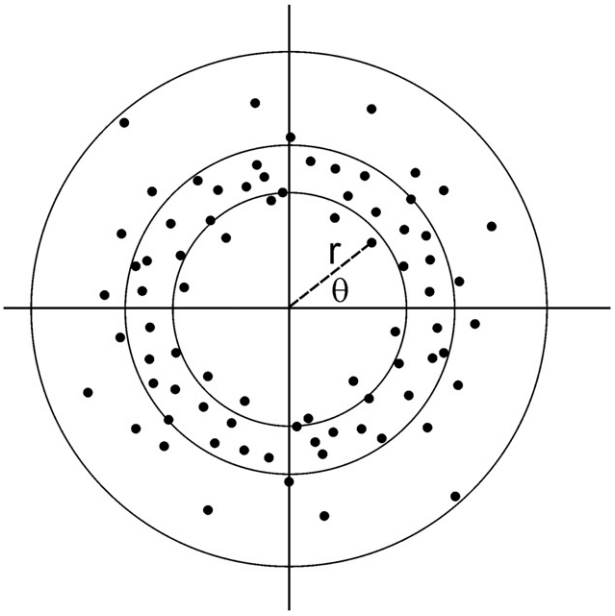

Fig. 2. Vector diagram of inter-point distances (Fry diagram). See text for explanation.

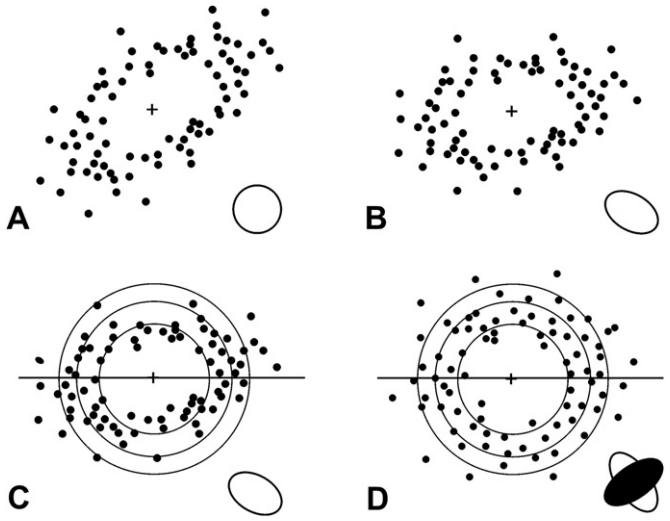

Fig. 3. Strain analysis method. A, The data plotted on Fry diagram. B, Trial de-straining applied. C, Isotropy and Poisson test applied to de-strained point pattern. D, An acceptable de-straining, strain ellipse in black.

program, *PointStrain,* which runs on a PC with Windows XP and is available on request from the author.

3.1. Analysis

The data consist of coordinates defining point positions. These positions are altered by each trial retrodeformation. A successful de-straining is one that returns the set of points to positions that accord with those assumed for the pre-deformation state. The assumption of initial isotropy is first examined by means of Kuiper's Test (Mardia, 1972). This test examines the uniformity of the points within each of the hoop sampling area (Fig. 3c, d) in terms of their angular spacing. Details are given in Appendix 1.

However isotropy alone is not sufficiently diagnostic of the de-strained state because random (Poisson) point distributions retain their isotropic character even after deformation (Fry, 1979). Therefore, a second statistical test detects the Poisson distribution of points. For a Poisson distribution of points across the vector diagram, the expected number of points falling within in a given sampling region is directly proportional to the area of that region (Fig. 2). In practice, the distribution of points is not uniform throughout the cells and deviations from uniformity are assessed by the Chi-squared Test, whose test statistic is given by

$$\chi^2 = \sum_{i=1}^{i=3}\left(O_i^2/E_i\right) - N, \qquad (1)$$

where N is the total number of points in all three hoop cells, O_i, E_i is the observed and expected number of points respectively in each of the three hoop areas. E_i is proportional to the area of the ith hoop area. The hypothesis that the dataset is a sample from a Poisson distribution is rejected when chi-square exceeds 5.991, the 0.95 critical value for 2 degrees of freedom.

In summary, a successful retrodeformation is recognized as one that returns an isotropic, but non-random, set of points. Typically more than 25,000 trial retrodeformations involving different combinations of strain ratio and orientation are applied (see Appendix 2 for details). Experience gained from analysis of many real and synthetic datasets shows that it is very rare for just one of these retrodeformations to be successful. In other words, a range of possible solutions to the strain analysis problem exists. In the following section we consider this issue further with reference to a number of examples.

4. Examples

4.1. Analysis of undeformed samples

Evaluation of the new method requires the analysis of samples corresponding to known tectonic strains. In this regard, the undeformed sedimentary grain data published by Waldron and Wallace (2007, their Fig. 9A) are useful. These data derive from a simulated accumulation of sedimentary grains with a predefined sorting. Samples with different degrees of anticlustering resulted from varying the grain sorting. The sequence of Samples A1–A4 (Waldron and Wallace, 2007; Fig. 8) corresponds to one of decreased grain sorting and hence decreasing anticlustering.

Using *PointStrain* to determine the strain in sample A1 (Fig. 4a), a strongly anticlustered point dataset with a high density halo on the Fry diagram (Fig. 4b), yielded a very restricted range of strain results centred around the known strain ratio, $R_s = 1$ (Fig. 4c, d). Of the 26,000 de-strainings applied to the dataset, only 61 produced point distributions compatible with the assumptions of isotropy. On the other hand, the less anticlustered dataset A3 (Fig. 4e, f) produced much broader strain estimates (Fig. 4g, h). For example, sample A3 produced 2208 strain solutions which, as well as including the condition of no strain ($R_s = 1$), also include strain ratios as high as $R_s = 1.45$.

The experiment reveals that point patterns can be considered a type of strain marker whose quality can vary greatly. In favourable circumstances with pronounced anticlustering, they are geometrically analogous to well defined circular markers that serve as precise strain gauges. In other instances, they are akin to strain markers that are not fully defined.

4.2. Analysis of artificially deformed samples

To evaluate the new strain analysis method, I subjected Waldron and Wallace's (2007, Fig. 7a) four undeformed point datasets with differing degrees of anticlustering (A1–A4) to simple shear transformations of dextral sense, horizontal shear direction and with two different shear strains ($g = 0.5$ and 1.0).

Sample A2 is relatively strongly anticlustered and yields a Fry diagram with a rather well defined central vacancy (Fig. 5a). The strains corresponding to those deformations that successfully restore the point data to an isotropic, but non-Poisson, fabric are represented as strain ellipses (Fig. 5b) and on a strain plot (Fig. 5c). The strain plot, devised by Elliott (1970), displays strain ellipses in polar coordinates (r, q) where r equals natural log of the axial ratio of the ellipse and q is the doubled angle of inclination of the ellipse long axis relative to some chosen reference line. Only 63 of the 33,000 trial de-strainings were successful, and they have a modal distribution in the strain plot. Therefore, a set of strain markers with this distribution would yield point populations that closely constrains the tectonic strain ellipse. In contrast, the deformed Sample A4 produces an ellipse on the Fry diagram with a fuzzy periphery (Fig. 5d). When these data are analyzed, it is found that 2227 of 30,000 yield a solution and they create a wide range of strains (Fig. 5e, f). In both simulations, the applied strain lies within the area of the strain plot that contains the successful de-strainings (Fig. 5c, f)

It is clear from this experiment that the proposed method delivers a range of solutions to the strain analysis problem and that the Elliott plot is useful representation of this range. Given the aim of deriving a best estimate strain from *PointStrain* program, a mean solution was calculated as the centre of gravity of the solution field on the Elliott plot. When calculating the mean strain, care needs to be taken to ensure that the trial de-strainings are arranged on a uniform grid in solution space (see Appendix 2).

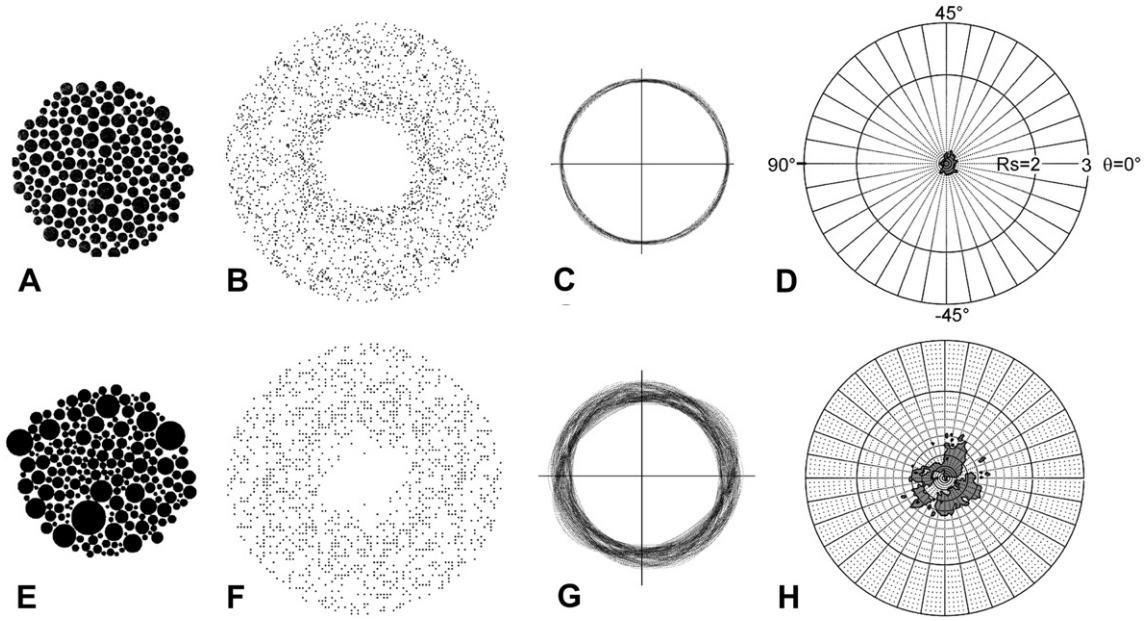

Fig. 4. Strain analysis of undeformed simulated samples. A, Sample of Waldron and Wallace (2007, Fig. 8a (i)); B, C, D, Fry plot, acceptable strain ellipses, Elliott plot of acceptable strains respectively. E, Sample of Waldron and Wallace (2007, Fig. 8a (iii)); F, G, H, Fry plot, acceptable strain ellipses, Elliott plot of acceptable strains respectively.

The mean solutions are generally close to the correct strain value (Table 1). The orientation of the mean strain lies within 2° of the correct value, and the error for the strain ratio varies from 1% to 12% and appears to be larger in weakly anticlustered samples.

4.3. Comparison with the results of the methods of Waldron and Wallace (2007)

Waldron and Wallace (2007) describe two alternative objective methods for determining the point fabric ellipse: the continuous function and the point-counting ellipse methods. They are based on the determination of the axial ratio of elliptical high density halo of points that is characteristic of anticlustered point data plotted on Fry diagrams. To assess the performance of their methods they analyze datasets of known strain (Waldron and Wallace, 2007, Table 2). For comparison with the present method, the same data were analyzed by the program *PointStrain* (Table 2).

Each strain estimate obtained by Waldron and Wallace (2007) and by the present study is compared to the corresponding known strain ellipse by calculating a new index that measures the

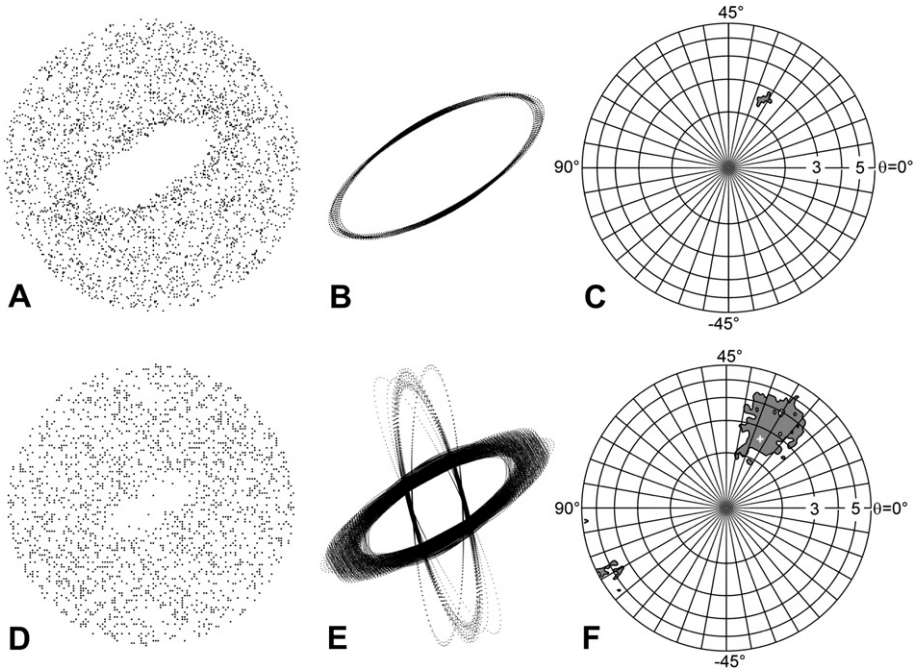

Fig. 5. Strain analysis from synthetic samples deformed by dextral simple shear with a shear strain of 1.0, corresponding to strain ellipse with $R = 2.62$ and $q = 32°$ (Table 1). A, B, C, Fry diagram, acceptable strain ellipses and Elliott plot of strain ellipses respectively for sample 2; D, E, F, Fry diagram, acceptable strain ellipses and Elliott plot of strain ellipses respectively for sample 4. The actual simulated strain ellipse is shown by the cross in D.

Table 1
Strain results obtained from synthetic grain-centre data (Waldron and Wallace, 2007, Fig. 8a) deformed by simple shear ($g = 0.5$, $g = 1.0$). Sorting and anticlustering decreases progressively from Samples 1 to 4. N_s is the number of solutions obtained. The average R_s and theta of these solutions are given.

	$\gamma = 0.5$ [$R_s = 1.64$, $\theta = 38°$]			$\gamma = 1.0$ [$R_s = 2.62$, $\theta = 32°$]		
	Mean (R_s, q)	Misfit	N_s	Mean (R_s, q)	Misfit	N_s
Sample 1	1.63, 37°	1.019	56	2.60, 32°	1.008	63
Sample 2	1.67, 37°	1.026	67	2.67, 31°	1.045	68
Sample 3	1.73, 36°	1.068	291	2.74, 30°	1.096	303
Sample 4	1.84, 39°	1.124	2181	2.83, 33°	1.091	2227

degree of incompatibility between two strain ellipses, termed here the misfit strain factor. The misfit factor is the axial ratio of the ellipse that results from the superimposition of one strain ellipse with the reciprocal strain ellipse of the second ellipse. The superimposition of two very similar ellipses would produce a near circular shape. Therefore, a misfit factor close to 1.0 indicates close similarity of the two ellipses, whereas larger values indicate greater difference. The procedure for calculating the misfit factor is outlined in Appendix 2. This misfit factor is calculated in Table 2 to assess the relative quality of the strain estimates from the different methods. The present method, the continuous function method and the point-counting ellipse method delivered mean misfit factors of 1.158, 1.377 and 1.251 respectively. Although based on a limited number of samples, the proposed method here delivers improved results as compared to these two techniques.

4.4. Analysis of real data: oolitic limestone

Ooid grain centres were digitized from the photomicrograph of oolitic limestone published by Ramsay and Huber (1983, Fig. 7.7) to provide a series of samples of different sizes. Sample sizes varying from 50 to 150 points were constructed from all grains lying within a predefined area of the image. Perhaps not surprisingly, the range of solutions for the strain decreases as the sample size increases (Fig. 6). For sample sizes of 50, 75, and 100, the average number of acceptable solutions is 448, 201, and 47, respectively. This is consistent with the expectation that a greater precision of strain determination can expected to be obtained by using larger sample sizes. With regard to the minimum sample size required for the method, the shape of the solution field on the Elliott plot is a useful indication of the reliability of the result. For example, the solutions for a sample size of 50 points (Fig. 6c) are so dispersed that any average solution is unlikely to be robust (Fig. 6d). On the other hand, we have more confidence in the compact pattern of results in Fig. 6b obtained when the sample size is 100 grain centres (Fig. 6a).

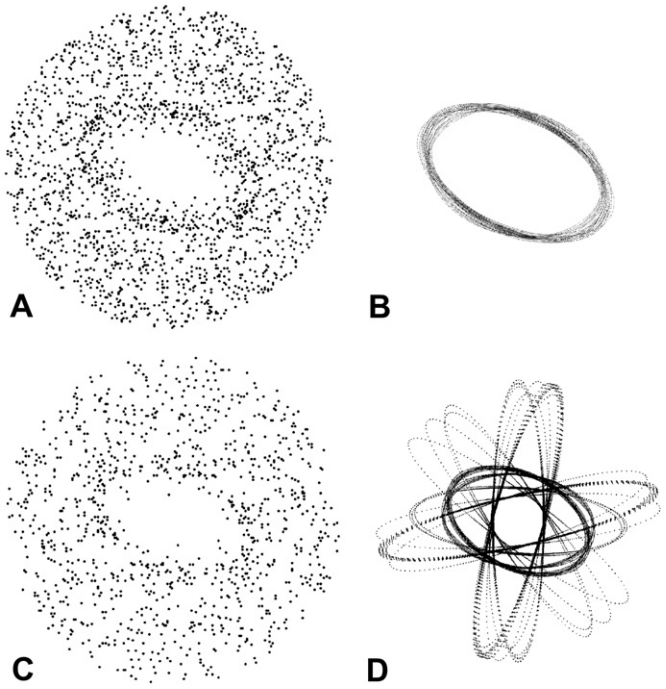

Fig. 6. The results of strain analysis of samples taken from Ramsay and Huber (1983, Fig. 7.7) for different sample sizes, N. A, B Fry plot and acceptable strain ellipses respectively for sample with $N = 100$. C, D, Fry plot and acceptable strain ellipses from sample with $N = 50$.

The analysis of the largest sample consisting of all discernable grain centres (257 points) produced an unexpected result. At the usual 95% significance level, no acceptable solutions were obtained, i.e., no de-straining was found that could restore the present point fabric to an isotropic one. This indicates that the basic requirements of the method are not being met in this sample. At the 97.5% level, only four solutions were found with an average strain ratio of 1.66 and strain direction of −25°, a result that is apparently compatible with the Fry diagram (Fig. 7a) and visual fit of Ramsay and Huber (1983, p. 120). By using this strain estimate to restore the point fabric, a probable explanation is found for this curious result. The restored Fry diagram (Fig. 7b) shows what appears to be a weak hexagonal point instead of the ideal circular. If real, such a point pattern may be expected from close packing of well-sorted grains, i.e. extreme degrees of anticlustering. This lack of initial isotropy would prevent a successful de-straining of the fabric to an isotropic condition.

Table 2
Comparison of results of present method with two methods of Waldron and Wallace (2007). N_s, number of acceptable solutions using 0.95 critical values for statistical tests and a grid-spacing with successive de-strainings having a misfit strain factor of 1.02.

Sample	N	Known strain: R_s, θ	Present method: R_s, θ	N_s	W & W Method 1: R_s, θ	W & W Method 2: R_s, θ
Fig 8b1	200	1.30, −48	1.23, −46	59	1.25, −54	1.32, −74
Fig 8b2	200	1.80, −57	1.75, −57	30	1.74, −58	2.04,−64
Fig 8b3	200	2.50, −13	2.48, −10	135	2.36, −13	2.12, −16
Fig 8c2	242	1.30, −48	1.52, −45	1976	1.39, −11	1.2, −61
Fig 8c3	239	1.80, −57	1.98, −53	1449	1.56, −38	1.63, −75
Fig 8c4	237	2.50, −13	2.45, −18	1364	3.84, −4	2.1,−10
Mean misfit factor			**1.159**		**1.377**	**1.251**

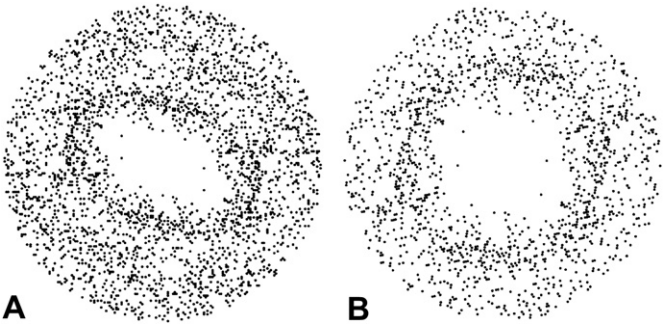

Fig. 7. Analysis of deformed oolitic limestone in Ramsay and Huber (1983, Fig. 7.7). 257 ooid centres. A, Fry diagram. B, restored Fry plot after removal of strain.

5. Conclusions

Fry's method for analyzing deformed point patterns has great appeal given its simplicity, novel design and for the visual appreciation it gives of the strain ellipse. However, in practice the visual selection of the best-fit strain ellipse is frequently a source of ambiguity.

This paper offers an alternative, objective computer-based technique for obtaining the best-fit strain ellipse by repeatedly destraining the point data to identify those strain states that are capable of restoring the data to assumed initial conditions, i.e. an isotropic but non-Poisson point distribution. The usual result of this process is to obtain a range of acceptable solutions to the strain analysis problem, and the number of solutions serves to place constraints on the strain ellipse's strain ratio and orientation. The plot of Elliott (1970) is useful for depicting the obtained range of solutions. Testing of the method with synthetic data simulated from pure and simple shear shows that the mean solutions produce strain estimates which compare favourable with other Fry-related methods.

In general, the strain ellipse is better constrained with data derived from strongly anticlustered point distributions. Weakly anticlustered point distributions that produce vague, poorly defined vacancy fields on the Fry diagram lead to a broad range of solutions with the new method.

The minimum sample size that can be dealt with the present method is about 75 points. This lower limit is imposed by the requirements of statistical tests used to detect isotropy of the restored point fabrics. In general, larger samples place closer constraints on the strain results.

Acknowledgements

Discussions over the years with former colleague Norman Fry were invariably stimulating. Mark McNaught, Kieran Mulchrone and editor Bill Dunne suggested useful improvements to the paper.

Appendix 1. The hoop diagram design and Kuiper's test

The hoop diagram in Fig. 2 is used for statistical testing of destrained point patterns. It is used to sample the points of the point fabric using the Kuiper's and Chi-square tests. There are three sampling cells; a central circle and two hoop cells. These cells examine the distribution of points in the inner part of the Fry point pattern; the part most sensitive to the strain. However, since the size of the central region of the Fry diagram of low point population depends on average point spacing and the degree of anticlustering, the radii of the sampling hoops are not fixed a priori but are determined on the basis of the pattern of the point set being analyzed. To ensure that the sample contains sufficient points for use of the Kuiper test of isotropy adjustment of the radii of the hoops is made until the circle contains 40 points, and the two hoops contain 80 and 120 points respectively.

Kuiper's Test (Mardia, 1972, pp. 173–180; Cheeney, 1983, pp. 95–97) is an efficient method for assessing the distribution of points within each cell of the hoop diagram. It tests the hypothesis that the points are uniformly distributed around the cell in the terms of the directions obtained by joining the points to the origin of the polar diagram (Fig. 2). For a perfect uniform distribution, the expected number of points encountered as we travel around the hoop, expressed as a proportion of total number in the hoop, is equal to the angle travelled as a proportion of the complete revolution. For a real sample, the points encountered during an angle of travel will differ from the prediction above, and the maximum discrepancy attained during complete revolution is the test statistic. If this maximum discrepancy is too large we can reject the hypothesis of a uniform distribution (see Mardia, 1972, p. 178). This test is well suited for the detection of strain effects, because strain will tend to produce large positive and negative discrepancies 90° apart.

Appendix 2. The misfit strain factor for two strain ellipses

Any comparison of a pair of strain ellipses needs to account for their difference of aspect ratio, R, as well as their difference of orientation. These two aspects need to be considered together because the significance of a given difference in orientation depends on the axial ratio of the ellipses involved. Here the misfit strain factor is proposed for this purpose.

The misfit strain factor between two strain ellipses is defined as the axial ratio of the strain ellipse that results from the superimposition of the first strain ellipse with the second strain ellipse, the second having been rotated through 90°. Two identical ellipses would produce a circle, giving a misfit factor 1.0.

Fig. A2.1 defines the variables required for the calculation of the misfit factor. A first and a second ellipse with axial ratios R_1 and R_2 respectively show an angular orientation difference of q. When the second ellipse is rotated through 90°, the orientation difference becomes $q' = q + 90°$. Using equations of Elliott (1970, eq. 23) and De Paor (1988, eq. A.14) we obtain the following equation for the axial ratio of the strain ellipse resulting from the superimposition of ellipse 1 and rotated ellipse 2:

$$R_{\text{misfit}} = \frac{1}{2}\left(K + \sqrt{K^2 - 4}\right), \tag{2}$$

where

$$K = 2\left(C_1 C_2 + S_1 S_2 \cos 2\theta'\right), \tag{3}$$

$$\cos 2\theta' = 2\sin^2 \theta - 1, \tag{4}$$

$$C = \frac{1}{2}(R + 1/R), \tag{5}$$

and

$$S = \frac{1}{2}(R - 1/R). \tag{6}$$

This index of difference between strains is used in two different ways in this study. Firstly, it is used to construct a uniform grid of the

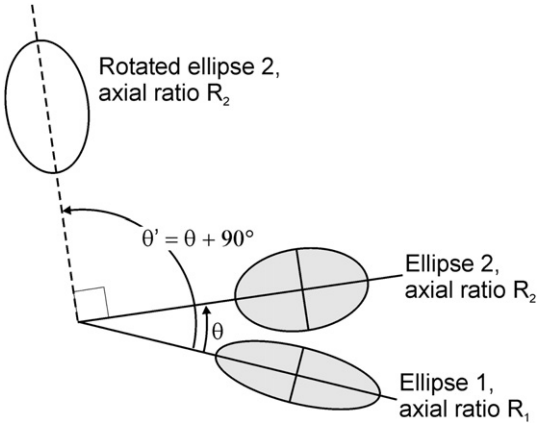

Fig. A2.1. The variables used in the calculation of the misfit strain factor, an index of difference between two strain ellipses with axial ratios R_1 and R_2 respectively, and difference of orientation q.

variables axial ratio and orientation for the systematic coverage of parameter space during the series of de-strainings of the point data. By arranging de-strainings with constant spacing in terms of R_{misfit}, the acceptable solutions can be averaged without bias. A uniform polar grid is used in which grid nodes are arranged on radial lines and concentric circles on the Elliott plot. The ellipses at neighbouring grid nodes always differ by a constant R_{misfit} value. Therefore, a suitable value of R_{misfit} is chosen a priori. Two ellipses corresponding to grid nodes that are radial neighbours have axial ratios R_1 and R_2 but have parallel orientation, i.e. $q = 0^\circ$. If R_1 is known, equations (2)–(6) are used to calculate the value of R_2. Similarly, two ellipses corresponding to grid nodes that are circumferential neighbours have different orientations but have axial ratios $R_1 = R_2$. If R_1 is known, equations (2)–(6) are used to calculate the value of q.

Secondly, R_{misfit} is used to compare the results of strain analysis with known strains or with results produced by the use of other methods.

References

Cartwright, A., Whitworth, A.P., 2008. The directional analysis of star clusters. Monthly Notices of the Royal Astronomical Society 390, 807–813.

Cheeney, R.F., 1983. Statistical Methods in Geology. George Allen and Unwin. 169pp.

Crespi, J.M., 1986. Some guidelines for the practical application of Fry's method of strain analysis. Journal of Structural Geology 8, 799–808.

De Paor, D.G., 1988. R_f/f_f strain analysis using an orientation net. Journal of Structural Geology 10, 323–333.

Elliott, D., 1970. Determination of finite strain and initial shape from deformed elliptical objects. Geological Society of America Bulletin 81, 2221–2236.

Erslev, E.A., 1988. Normalized center-to-center strain analysis of packed aggregates. Journal of Structural Geology 10, 201–209.

Fry, N., 1979. Random point distributions and strain measurement in rocks. Tectonophysics 60, 89–105.

Genier, F., Epard, J.-L., 2007. The Fry method applied to an augen orthogneiss: problems and results. Journal of Structural Geology 29, 209–224.

Hanna, S.S., Fry, N., 1979. A comparison of methods of strain determination in rocks from southwest Dyfed (Pembrokeshire) and adjacent areas. Journal of Structural Geology 1, 155–162.

Lacassin, R., van der Driessche, J., 1983. Finite strain determination of neiss: application of Fry's method to porphyroid in the Southern Massif Central (France). Journal of Structural Geology 3, 245–253.

Mardia, K.V., 1972. Statistics of Directional Data. Academic Press, London.

McNaught, M.A., 2002. Modifying the normalized Fry method for aggregates of non-elliptical grains. Journal of Structural Geology 16, 493–503.

Ramsay, J.G., 1967. Folding and Fracturing of Rocks. McGraw-Hill Book Company, New York.

Ramsay, J.G., Huber, M.I., 1983. The techniques of modern structural geology. In: Strain Analysis, vol. 1. Academic Press.

Schwerdtner, W.M., Stott, G.M., Sutcliffe, R.H., 1983. Strain patterns in crescentic granitoid plutons in the Archean greenstone terrain of Ontario. Journal of Structural Geology 5, 419–430.

Treagus, S.H., Treagus, J.E., 2002. Studies of strain and rheology of conglomerates. Journal of Structural Geology 24, 1541–1567.

Vearncombe, J., Vearncombe, S., 1999. The spatial distribution of mineralization; applications of Fry analysis. Economic Geology 94, 475–486.

Waldron, J.W.F., Jensen, L.R., 1985. Sedimentology of the Goldenville formation, Easter Shore, Nova Scotia. Geological Survey of Canada Paper 85-15.

Waldron, J.W.F., Wallace, K.D., 2007. Objective fitting of ellipses in the centre-to-centre (Fry) method of strain analysis. Journal of Structural Geology 29, 1430–1444.